HAL
archives-ouvertes.fr

Theoretical description of the photorefractive detection of the ultrasound modulated photons in scattering media

Michel Gross, François Ramaz, B.C. Forget, Michael Atlan, Albert-Claude Boccara, Philippe Delaye, Gérald Roosen

▶ **To cite this version:**

Michel Gross, François Ramaz, B.C. Forget, Michael Atlan, Albert-Claude Boccara, et al.. Theoretical description of the photorefractive detection of the ultrasound modulated photons in scattering media. Optics Express, Optical Society of America, 2005, 13 (18), pp.7097-7112. hal-00671127

HAL Id: hal-00671127
https://hal-iogs.archives-ouvertes.fr/hal-00671127

Submitted on 16 Feb 2012

HAL is a multi-disciplinary open access archive for the deposit and dissemination of scientific research documents, whether they are published or not. The documents may come from teaching and research institutions in France or abroad, or from public or private research centers.

L'archive ouverte pluridisciplinaire **HAL**, est destinée au dépôt et à la diffusion de documents scientifiques de niveau recherche, publiés ou non, émanant des établissements d'enseignement et de recherche français ou étrangers, des laboratoires publics ou privés.

Theoretical description of the photorefractive detection of the ultrasound modulated photons in scattering media

M. Gross
Laboratoire Kastler-Brossel, UMR 8552 (ENS, CNRS, UMPC), Ecole Normale Supérieure, 24 rue Lhomond F-75231 Paris cedex 05
gross@lkb.ens.fr

F. Ramaz, B.C. Forget, M. Atlan, A.C. Boccara
Laboratoire d'Optique, Ecole Supérieure de Physique et de Chimie Industrielles de la Ville de Paris, CNRS UPRA0005, Université Pierre et Marie Curie, 10 rue Vauquelin F-75231 Paris cedex 05
ramaz@optique.espci.fr

P. Delaye, G. Roosen
Laboratoire Charles Fabry de l'Institut d'Optique, Unite Mixte de recherche du Centre National de la Recherche Scientifique, de l'Institut d'Optique et de l'Univeristé Paris-Sud, Bat 503, Centre Scientifique d'Orsay F-91403 Orsay Cedex

Abstract: Acousto-optic imaging of thick biological tissues can be obtained in *real-time* with an *adaptive-wavefront* holographic setup, where the holographic media is a self-developping photorefractive crystal. As a consequence, the interference signal resulting from the acousto-optic effect can be easily collected with a high *etendue* and fast single photodetector. We present a statistical model of the field propagating through the scattering media and show why the various acoustic frequency components contained in the speckle output pattern are uncorrelated. We then give a detailed description of the signal measured through the photorefractive effect, in order to explain the quadratic pressure response observed for the two commonly used configurations setup *e.g* an amplitude or a phase modulation of the ultrasound.

© 2005 Optical Society of America

OCIS codes: (170.1650) Coherence imaging; (170.3660) Light propagation in tissues; (290.7050) Turbid media; (090.0090) Holography; (090.2880) Holographic interferometry; (170.7050) Turbid media

References and links

1. L. Wang, S. Jacques, and X. Zhao, "Continuous wave ultrasonic modulation of scattered light to image objects in turbid media." Opt. Lett. **20**, 629 (1995).
2. A. Kak and M. Slaney, *Principles of Computerized Tomographic Imaging* (IEEE Press, New York., 1988).
3. W. Leutz and G. Maret, "Ultrasonic modulation of multiply scattered light," Physica B **204**, 14 (1995).
4. M. Kempe, M. Larionov, D. Zaslavsky, and A. Z. Genack, "Acousto-optic tomography with multiple scattered light," J. Opt. Soc. Am. B **14**, 1151–1158 (1997).
5. L. Wang, "Mechanisms of ultrasonic modulation of multiply scattered coherent light: a analytic model," Phys. Rev. Lett. **87**, 1 (2001).

#7601 - $15.00 USD Received 25 May 2005; revised 12 July 2005; accepted 29 August 2005
(C) 2005 OSA

6. A. Lev and B. Sfez, "in vivo demonstration of ultrasound-modulated light technique," J. Opt. Soc. Am. A **20**(12), 2347–2354 (2003).
7. M. Gross, P. Goy, B. C. Forget, M. Atlan, F. Ramaz, A. C. Boccara, and A. K. Dunn, "Heterodyne detection of multiply scattered monochromatic light with a multipixel detector," to appear in Opt. Lett. (2005).
8. A. Lev, Z. Kotler, and B. Sfez, "Ultrasound tagged light imaging in turbid media in a reflectance geometry," Opt. Lett. **25**, 378 (2000).
9. S. Lévêque, A. C. Boccara, M. Lebec, and H. Saint-Jalmes, "Ultrasonic tagging of phton paths in scattering media: parallel speckle modulation processing," Opt. Lett. **24**(3), 181 (1999).
10. M. Gross, P. Goy, and M. Al-Koussa, "Shot-noise detection of ultrasound-tagged photons in ultrasound-modulated optical imaging," Opt. Lett. **28**(24) (2003).
11. T. W. Murray, L. Sui, G. Maguluri, R. A. Roy, A. Nieva, F. Blonigen, and C. A. DiMarzio, "Detection of ultrasound-modulated photons in diffuse media using the photorefractive effect," Opt. Lett. **29**(21), 2509 (2004).
12. F. Ramaz, B. C. Forget, M. Atlan, A. C. Boccara, M. Gross, P. Delaye, and G. Roosen, "Photorefractive detection of tagged photons in ultrasound modulated optical tomography of thick biological tissues," Opt. Express **12**(22), 5469–5474 (2004).
13. E. Bossy, L. Sui, T. W. Murray, and R. A. Roy, "Fusion of conventional ultrasound imaging and acousto-optic sensing by use of a standard pulsed-ultrasound scanner," Opt. Letters **30**(7), 744 (2005).
14. F. J. Blonigen, A. Nieva, C. DiMarzio, S. Manneville, L. Sui, G. Maguluri, T. W. Murray, and R. A. Roy, "Computations of the acoustically induced phase shifts of optical paths in acoustophotonic imaging with photorefractive-based detection," Appl. Opt. **44**(18), 3735 (2005).
15. L. Sui, R. A. Roy, C. DiMarzio, and T. W. Murray, "Imaging in diffuse media with pulsed-ultrasound-modulated light and the photorefractive effect," Appl. Opt. **44**(19), 4041 (2005).
16. M. Atlan, B.C. Forget, F. Ramaz, A.C. Boccara, and M. Gross, "Pulsed acousto-optic imaging in dynamic scattering media with heterodyne parallel speckle detection," Opt. Lett. **30**(11), 1360–1362 (2005).
17. L. Wang, "Mechanisms of ultrasonic modulation of multiply scattered coherent light: a Monte Carlo model," Opt. Lett. **26**, 1191 (2001).
18. P. Delaye, L. A. de Montmorillon, and G. Roosen, "Transmission of time modulated optical signals throug an absorbing photorefractive crystal," Opt. Commun. **118**, 154 (1995).
19. A.Hermanns, C.Benkert, D.M.Lininger, and D.Z.Anderson, "The transfer function and impulse response of photortefractive two beam coupling," IEEE J. Quantum Electron. **28**, 750 (1992).
20. F.M.Davidson and C. Field, "Coherent homodyne optical communication receivers with photorefractive optical combiners," J. Lightwave Technol. **12**, 1207 (1994).
21. A. L. an B. G. Sfez, "Direct, noninvasive detection of photon density in turbid media," Opt. Lett. **27**(7), 473 (2002).
22. L. Solymar, D. Webb, and A. Grunnet-Jepsen, *The physics and applications of photorefractive materials* (Clarendon Press, Oxford, 1996).
23. A. Yariv, *Quantum electronics* (John Wiley and Sons, New York, 1989).
24. G. Hamel de Montchenault and J.P.Huignard, "Two-wave mixing with time-modulated signal in $Bi_{12}SiO_{20}$ theory and application to homodyne wave-front detection," J. Appl. Phys. **63**, 624 (1988).
25. I.Lahiri, L. Pyrak-Nolte, D.D.Nolte, M. Melloch, R. Kruger, G. Bacher, and M. Klein, "Laser-based ultrasound detection using photorefractive quantum wells," Appl. Phys. Lett. **73**, 1041 (1998).
26. D. Webb and L.Solymar, "Amplification of temporally modulated signal beams by two-wave mixing in $Bi_{12}SiO_{20}$," J. Opt. Soc. Am. B **7**, 2369 (1990).
27. S.Bian and J.Frehlich, "Phase modulated two wave mixing in crystals with long photocarriers lifetimes," J. Mod. Opt. **43**(1185) (1996).
28. L. A. de Montmorillon, P. Delaye, J. Launay, and G. Roosen, "Novel theoretical aspects on photorefractive ultrasonic detection and implementation of a sensor with an optimum sensitivity," J. Appl. Phys. **82**, 5913–5922 (1997).
29. P. Delaye, S. de Rossi, and G. Roosen, "Photorefractive vibrometer for the detection of high amplitude vibrations on rough surfaces," J. Opt. A: Pure and Applied Optics **2**, 209–215 (2000).
30. P. Delaye, A. Blouin, D. Drolet, L. A. de Montmorillon, G. Roosen, and J. Monchalin, "Detection of ultrasonic motion of a scattering surface by photorefractive InP :Fe under an applied dc field," J. Opt. Soc. Am. B **14**(7), 1723 (1997).
31. P. Delaye and G. Roosen., "Evaluation of a photorefractive two beam coupling novelty filter," Opt. Commun. **165**, 133–151 (1999).

1. Introduction

Ultrasound modulated optical imaging [1] combines light and ultrasound to image optical contrast in thick and highly scattering media with the spatial resolution of ultrasound imaging. This technique is promising for biomedical applications, for example breast imaging, for which

#7601 - $15.00 USD Received 25 May 2005; revised 12 July 2005; accepted 29 August 2005
(C) 2005 OSA

optical imaging techniques (such as Diffuse Optical Tomography [2]) can provide significant functional information but are generally limited to a poor spatial resolution.

The principle is the following. A coherent (laser) light source illuminates a highly scattering sample. Due to the scattering, the photons will travel along of great number of random paths, producing a speckle pattern. At the same time, an ultrasound (US) beam is focused in the sample. Some of the travel paths, those crossing the US focal area, will be modulated due to the movement of scatterers [3–5] and to the local change in the refractive index [5]. This partial phase-modulation of the outcoming field leads to a modulation of the intensity of the speckle pattern at the US frequency. This corresponds to the "tagged photons", which are emitted, in the diffused light frequency spectrum, within acoustic sidebands. Measuring the weight of the tagged photon component as a function of the location of the US focal point allows to get 3D images of the scattering medium.

The detection of the tagged photon is difficult. The signal is weak, and spatially incoherent (speckle). Moreover, the parasitic motion of the scatterers, related to the blood *flux* in the *in vivo* case, decorrelates the speckle in a relatively short time. This corresponds *in vivo* to a spectral broadening in the kHz range [6,7]. Many techniques have been used to detect the tagged photons. First, experiments have been done with a photodiode which records the modulation of the speckle at the US frequency [1, 8]. The optical *etendue* (product of the detector area by the detection solid angle) is low because one detects only one or a few speckle grains, but since the detector is fast, all the tagged photons in the optical *etendue* can be detected, whether the spectrum is broad or not. To increase the *etendue*, a CCD camera can be used to detect many speckle grains in parallel. To get a slow modulation component compatible with CCD detection, Leveque et al [9] use a stroboscopic illumination technique, while Gross et al [10] perform heterodyne detection with the CCD. The latter allows to get optimal detection sensitivity (shot noise). However, both Leveque and Gross techniques are slow and narrow band, and they cannot detect all the tagged photons when the spectrum is broad, like in the *in vivo* case.

A novel technique, based on two wave mixing in a photorefractive (PR) crystal has been introduced recently [11–15]. This technique, which allows to detect the tagged photons with a higher *etendue* than with the CCD parallel detection, is potentially able to be fast enough to detect all the tagged photons in an *in vivo* sample. In the Murray et al variant of the technique [11], a beam splitter on the main laser provides the pump beam of the PR crystal. The pump is thus resonant with the "un tagged" photons, which are detected by PR effect. The "tagged photon" are seen indirectly, like in a spectroscopic absorption experiment, through a decrease of the "un tagged" photon signal DC component [14]. To get resolution along the US propagation z axis, the US beam is pulsed, and the signal is detected by a fast avalanche photodiode (APD). By scanning the US focus spot along the transverse x axis, tomographic 2D images are obtained [13, 15]. In the Ramaz et al variant of the technique [12], acousto optic modulators allow to freely adjust the amplitude, the phase and the frequency of the pump beam. By tuning the pump frequency resonant with the "tagged", or with the "un tagged" photons, it is possible to detect with the same setup either the "tagged" or the "un tagged" photons. In the first experiment [12], the "tagged photon" are detected, and the photodiode (PD) photoelectrons are amplified by a high impedance ($R = 10^6 \Omega$), and thus low noise, transimpedance amplifier, which is quite slow. No attends is made to get z resolution, and 1D "image" (or plot) are presented (like in the first Murray's experiment [11]). It may be possible to get z resolution (and to make thus 2D images) by pulsing both the US and the pump beams as done in [16].

It is not possible to decide yet which of the Murray's and Ramaz's techniques is the best, because the corresponding experiments are done with setups whose performances are very different. Murray et al use a slow BSO crystal (PR time $\tau_{PR} = 150\ ms$) with a fast APD photo-

#7601 - $15.00 USD Received 25 May 2005; revised 12 July 2005; accepted 29 August 2005
(C) 2005 OSA

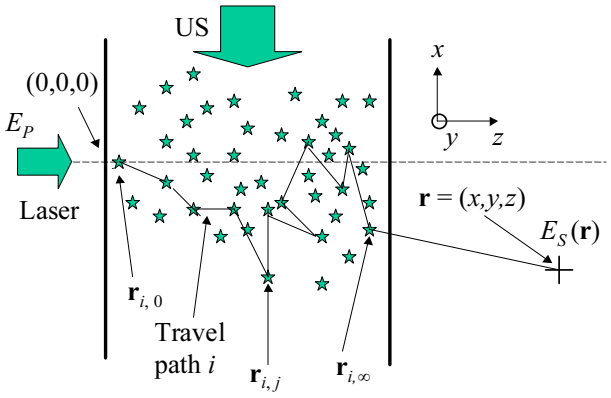

Fig. 1. Diffusion of light by scatterers (star).

detector, and do experiment with phantoms. Ramaz et al use a faster ($\tau_{PR} = 5\ ms$) GaAs crystal (which is still slow with respect to the need for *in vivo* imaging: $\tau_{PR} < 1ms$) with a slow photo-detector (PD), whose noise is low (because the impedance R is high), and do experiment with chicken sample ($2cm$ and $4cm$ width), closer to the breast imaging need.

Although many theoretical works have been done to describe both the acousto-optic imaging [3–5, 17], and the PR effect [18–20], there is no theoretical attends to describe the PR effect in the context of the acousto optic imaging (except of the very recent Blonigen et al. study [14]). The purpose of this paper is to give such a global description. Moreover, to get better understanding of the physical phenomena, the model must be able to describe both the Murray, and Ramaz experiments, and to deal with new possible configurations of these setups, not yet implemented.

In section 2, we will first model the scattered light outgoing the sample, and discuss its statistical properties. We will then show, in section 3, that it is possible to separate the so-called "tagged" field, which results from the interaction of the photons with ultrasound, from the "un tagged" field, since these fields do not oscillate at the same frequency. Moreover these fields are spatially incoherent. In section 4, we will consider the photorefractive effect performed with these two fields, and in section 5, the detection of the photorefractive signal on a large area photodiodes. We will got then a general expression for the PR signal (Eq. (31)). In order to verify the validity of our theoretical model, we will consider different types of ultrasonic modulations, *e.g* a phase or an amplitude modulation. They are discussed in detail in section 6. Finally, experimental validation of the model is presented in section 7 and we give as a comparison a Fourier spectrum of the signal in the case of amplitude and phase modulation of the US at $1500Hz$.

2. The fields observed with and without ultrasound

Let us call E_P and E_S the fields coming into and out of the sample. Consider the point (x,y) located after the sample output interface. E_S is a quasi monochromatic wave at the frequency ω_0 of the incoming laser. Let us introduce the complex field amplitude $\mathscr{E}_S$ defined as:

$$E_S(\mathbf{r},t) = \boldsymbol{Re}\left(\mathscr{E}_S(\mathbf{r},t)e^{j\omega_0 t}\right) \tag{1}$$

Here ***Re*** is the real part operator. $\mathscr{E}_S$ results from the sum (or the interference) of the field components $\mathscr{E}_{S,i}$ scattered through the sample along many travel paths i from input plane ($z = 0$)

#7601 - $15.00 USD Received 25 May 2005; revised 12 July 2005; accepted 29 August 2005
(C) 2005 OSA

to the point ($\mathbf{r} = (x,y,z)$) (see Fig. 1).

$$\mathscr{E}_S(\mathbf{r},t) = \sum_i \mathscr{E}_{S,i}(\mathbf{r},t) \tag{2}$$

It is out of the scope of the paper to define more precisely the travel paths, and the summation over them. One can model, for example, the travel pathes by a Monte Carlo simulation.

For the travel path i, let us call a_i the weight of the scattered field component, and s_{i0} the travel path length. In s_{i0}, the zero index means that we do not yet consider the possible motions of the scatterers. Thus s_{i0} does not depend on time, and neither do $\mathscr{E}_{S,i}$ and $\mathscr{E}_S$. To simplify the description, without losing generality, we will consider that the phase of $\mathscr{E}_{S,i}$ depends only on travel path length (the change of phase associated to each scattering event is either neglected or included within s_{i0}):

$$\mathscr{E}_{S,i}(\mathbf{r}) = a_i(\mathbf{r}) e^{-j\theta_i(\mathbf{r})} \qquad \text{with} \qquad \theta_i(\mathbf{r}) = k\, s_{i0}(\mathbf{r}) \bmod (2\pi) \tag{3}$$

where mod is the modulo operator, and $k = 2\pi/\lambda$ the optical wave vector for the scattering medium. Since the travel paths length s_{i0} is large ($s_{i0} > z \gg \lambda$), and since the s_{i0} distribution is broad, θ_i is random and evenly distributed over the $[0...2\pi]$ interval from one travel path to the next. The travel pathes summation $\sum_i$ in Eq. (2) is thus equivalent to the step summation made to describe a random walk in the complex plane. The field $\mathscr{E}_S$ that results of this random walk is then a random quantity that obeys to a gaussian statistic.

We must notice that s_{i0} varies with the distance from the location $\mathbf{r}_{i,\infty}$ of the last scatterer to the considered point $\mathbf{r}$ following:

$$s_{i0}(\mathbf{r}) = s_{i0}(\mathbf{r}_{i,\infty}) + |\mathbf{r} - \mathbf{r}_{i,\infty}| \tag{4}$$

Substituting Eq. (4) into Eq. (3), we get that both $\mathscr{E}_{S,i}(\mathbf{r})$ and $\theta_i(\mathbf{r})$ vary rapidly with $\mathbf{r}$. The resulting $\mathscr{E}_S$ also varies fast with $\mathbf{r}$. This illustrates the speckle character of $\mathscr{E}_S$: θ_i varies thus in the x and y direction over distances that correspond to the speckle grain size. This property is important for θ_i, because it will allow us later to simplify Eq. (28) by making $i = i'$.

Let us now apply a CW (Continuous Wave) ultrasonic (US) wave to the system by using an ultrasonic piezoelectric (PZT) device. The PZT excitation voltage is simply:

$$U_{PZT}(t) = \boldsymbol{Re}\left(\mathscr{U}_{PZT}(t)\, e^{j\omega_{US}t}\right) \tag{5}$$

Here $\mathscr{U}_{PZT}$ is the PZT voltage complex amplitude with respect to the ω_{US} frequency. To simplify the description, we will consider in the following that the PZT voltage $\mathscr{U}_{PZT}$ is low enough to have an acoustic pressure proportional to $\mathscr{U}_{PZT}$. We have verified experimentally (with an hydrophone) that all the results presented here correspond to this regime.

To account possible schemes of US modulation $\mathscr{U}_{PZT}$ may depend on time, but varies slowly with respect to ω_{US}. Under the combined effect of the US motion of the scatterers, and the US modulation of the medium refractive index, the length s_i of the travel path i change periodically at the US frequency.

$$s_i(\mathbf{r},t) = s_{i0}(\mathbf{r}) + \boldsymbol{Re}\left(\delta s_i(t)\, e^{j\omega_{US}t}\right) \tag{6}$$

$$\beta_i(t) = k|\delta s_i(t)| \qquad\qquad \phi_i(t) = \arg\left(\delta s_i(t)\right) \tag{7}$$

where arg is the complex argument. Here, $\delta s_i = (\beta_i/k, \phi_i)$ is the modulated component of the travel path length s_i in complex representation. β_i, which is an angle, is the corresponding modulation of the optical phase. δs_i, β_i and ϕ_i are slowly varying with time (with respect to ω_{US}). δs_i (and thus β_i) is proportional to the acoustic pressure. δs_i results of the sum of the

#7601 - $15.00 USD Received 25 May 2005; revised 12 July 2005; accepted 29 August 2005
(C) 2005 OSA

modulations $\delta s_{i,j}$ induced all along the travel path, on the locations $\mathbf{r}_j$ of each scatterers j (see Fig. 1).

$$\delta s_i(t) = \sum_j \delta s_{i,j}(t) \tag{8}$$

On each scatterer, the phase of $s_{i,j}$, which is slowly varying with time, depends on the phase of the US beam at $\mathbf{r}_j$. Because of the "banana" shape of the photon density inside the scattering medium [21], the extension Δx of the travel pathes in the x direction is much larger than the US wavelength λ_{US} ($\Delta x \gg \lambda_{US}$). The phase of the US, and the phase of the local modulation $\delta s_{i,j}$ explore thus all phases of the $[0, 2\pi]$ interval. As a consequence, the summation made in Eq. (8) is equivalent to a 2D random walk in the complex plane, and δs_i is a random complex quantity.

The phase ϕ_i is thus random, and is equally distributed over the $[0, 2\pi]$ interval. Because the last scatterer, which is located near the sample output surface in $r_{j,\infty}$, does not move (or because its motion can be neglected), ϕ_i do not depend on $\mathbf{r}$ (contrarily to $\theta_i(\mathbf{r})$). This will simplify the final expression of the detected signal.

3. Decomposition of the transmitted field in Fourier components (CW ultrasonic excitation)

The periodic change of the travel path length s_i at the US frequency (Eq. (6)) can be written as :

$$s_i(\mathbf{r},t) = s_{i0}(\mathbf{r}) + \delta s_i(t)\ \sin(\omega_{US} t + \phi_i(t) + \pi/2) \tag{9}$$

Substituting $s_i(\mathbf{r},t)$ in Eq. (1) and Eq. (3), we get :

$$\mathscr{E}_{S,i}(\mathbf{r},t) = \ a_i(\mathbf{r}) e^{-j\theta_i(\mathbf{r})} e^{j\ \beta_i(t)\ \sin(\omega_{US} t + \phi_i(t) + \pi/2)} \tag{10}$$

Using the Fourier's expansion for the $e^{j\beta_i \sin(\omega_{US} t \ldots)}$ factor, we can develop the field $\mathscr{E}_{S,i}$, propagating along the travel path i, in Fourier components $\mathscr{E}_{S,i,\omega_n}$ (with respect to the ultrasonic modulation):

$$\mathscr{E}_{S,i}(\mathbf{r},t) = \sum_n \mathscr{E}_{S,i,\omega_n}(\mathbf{r})\ e^{jn\omega_{US} t} \tag{11}$$

$$\mathscr{E}_{S,i,\omega_n}(\mathbf{r}) = a_i(\mathbf{r})\ e^{-j\theta_i(\mathbf{r})}\ J_n(\beta_i(t))\ e^{jn(\phi_i(t)+\pi/2)} \tag{12}$$

In typical experimental situation, the US excitation is quite low, and $\beta_i \ll 1$. The field E_S is then a sum of Fourier components $\mathscr{E}_{S,\omega_n}$ of frequency $\omega_n = \omega_0 + n\omega_{US}$:

$$E_S(\mathbf{r},t) = \boldsymbol{Re}\ (\sum_n \mathscr{E}_{S,\omega_n}(\mathbf{r})\ e^{j\omega_n t}) \qquad \text{with} \qquad \mathscr{E}_{S,\omega_n}(\mathbf{r}) = \sum_i \mathscr{E}_{S,i,\omega_n}(\mathbf{r}) \tag{13}$$

The Eq. (13) will be used in the following to develop of the PR signal in Fourier components in Eq. (28). The general expression for the travel path field Fourier components of Eq. (12) will be used then to simplify Eq. (28) in order to get the final general expression for the signal (i.e. Eq. (31)). For practical use, we will consider mainly the $n = 0$ and $n = 1$ Fourier components, i.e. the "carrier" component ($n = 0$), which corresponds to the "un tagged" photons, and the first "sideband" component ($n = 1$), which corresponds to the "tagged" photons. We get:

$$\mathscr{E}_{S,\omega_0}(\mathbf{r}) = \sum_i a_i(\mathbf{r})\ e^{-j\theta_i(\mathbf{r})}\ J_0(\beta_i(t)) \tag{14}$$

$$\mathscr{E}_{S,\omega_1}(\mathbf{r}) = \sum_i a_i(\mathbf{r})\ e^{-j\theta_i(\mathbf{r})}\ J_1(\beta_i(t))\ e^{j(\phi_i(t)+\pi/2)} \tag{15}$$

Compare the phases of the i^{th} terms of the Eq. (14) and Eq. (15) summations. These phases differ by a factor $e^{j(\phi_i+\pi/2)}$ which is random (ϕ_i is random) from one travel path to the next. As a consequence, the fields $\mathscr{E}_{S,\omega_0}$ and $\mathscr{E}_{S,\omega_1}$, which results from 2 statistically independent random walks (Eq. (14) and Eq. (15)), are uncorrelated (i.e. optically spatially incoherent).

#7601 - $15.00 USD Received 25 May 2005; revised 12 July 2005; accepted 29 August 2005
(C) 2005 OSA

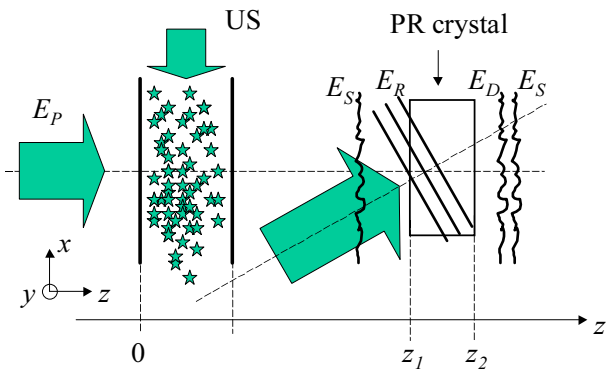

Fig. 2. Photorefractive interferometer.

4. The photorefractive (PR) effect on the tagged and un-tagged photons

The principle of the photorefractive (PR) interferometer is shown on Fig. 2. The signal beam E_S (tagged or un-tagged by the ultrasound) issued from the scattering media is collected by large numerical aperture (NA) lenses, and focused into a PR crystal. The E_S wavefront is highly distorted. In order to extract the desired information, a coherent reference beam E_R, called also the pump beam, interferes with the signal beam into the PR crystal. The reference beam E_R will be considered as a plane wave (this condition is not necessary but it simplifies the notations). The reference and the signal beams, which interfere within the photorefractive crystal, create through the photorefractive effect an hologram (or a grating) corresponding to a little change δn of the crystal complex refractive index (i.e. refractive index, and/or absorption) [22,23]. The PR effect having a finite response time, only the static components of the interference pattern (i.e. moving with frequency smaller than the inverse of the response time τ_{PR} of the crystal) will participate to the hologram inscription process. If the signal beam E_S has several frequency components, the PR effect selects the components whose frequencies are close the frequency of E_R. The pump beam is then diffracted by the PR holographic grating. The diffracted beam E_D has then the same wavefront than the signal beam E_S, which has written the hologram. E_D goes out the crystal, and propagates in the same direction as E_S [18–20, 24–27].

To make a quantitative analysis of the PR detection, we have to introduce the complex field amplitudes ε_R and ε_S with respect to the frequency ω of the reference pump beam E_R, which plays here the central role (and may differ from ω_0 depending on the implementation [11,12]).

$$E_R(\mathbf{r},t) = \boldsymbol{Re}\,(\varepsilon_R(\mathbf{r})\,e^{j\omega t}) \qquad E_S(\mathbf{r},t) = \boldsymbol{Re}\,(\varepsilon_S(\mathbf{r},t)\,e^{j\omega t}) \tag{16}$$

ε_R is constant, and ε_S, which contains all the ω_n frequency components, is time varying, we have from Eq. (13).

$$\varepsilon_S(\mathbf{r},t) = \sum_n \mathscr{E}_{S,\omega_n}(\mathbf{r})\,e^{j(\omega_n-\omega)t} \tag{17}$$

Two wave mixing in a photorefractive media with a constant pump beam ε_R, and a time varying (in amplitude and/or phase) optical signal beam ε_S, has been described in [18, 28]. The signal field $\varepsilon_S(x,y,z)$ within the crystal, i.e. for $z_1 < z < z_2$ (where $z = z_1$ and $z = z_2$ are the crystal input and output plane), can be written as a function of the crystal incoming field $\varepsilon_S(x,y,z_1)$, which is supposed to be known:

$$\varepsilon_S(x,y,z,t) = e^{-\alpha(z-z_1)/2}\left[\varepsilon_S(x,y,z_1,t) + \int_0^t dt'\,\varepsilon_S(x,y,z_1,t')\,G(z,t-t')\right] \tag{18}$$

#7601 - $15.00 USD Received 25 May 2005; revised 12 July 2005; accepted 29 August 2005
(C) 2005 OSA

$G(z,t)$ is given in [28]. In the condition of low efficiency of the grating and low absorption α of the crystal the transfer function $G(z,t)$ takes the simple form:

$$G(z,t) = (\gamma(z-z_1)/\tau_{PR})e^{-t/\tau_{PR}} \tag{19}$$

Here τ_{PR} is the response time of the photorefractive crystal and γ the photorefractive gain (that can be complex values in the more general modelling, but that are taken real in the present calculation, in accordance with the experimental conditions we use). In Eq. (18), $t = 0$ is the time origin, at which it is supposed that no hologram is written.

Equation (18) is established using several approximation that we will recall here [18]. The first one, is that we suppose that the pump beam is a constant monochromatic wave of pulsation ω (i.e. it is not time modulated). It is not perturbed by the grating, but it can lose its energy due to the crystal absorption. The pump beam intensity is also supposed to be much higher than signal beam intensity. The total incident illumination that governs the response time of the photorefractive crystal [22,23] is thus equal to the pump beam intensity. The response time that appears in the expression of $G(z,t)$ is the response time of the crystal taken at the entrance of the photorefractive crystal at position $z = z_1$. The model is established for two incident plane waves but it is immediately generalized to a speckled signal wave, that will be written into its plane wave decomposition, each plane wave being treated independently and the transmitted wave being the linear recomposition of the different transmitted plane wave components.

Since we are mainly interested by the solution of Eq. (18) with a periodic source term $\varepsilon_S(x,y,z_1,t)$, we may extend the lower limit of the $\int dt'$ integral of Eq. (18) from $t' = 0$ to $t' = -\infty$. Our purpose is to the make the periodicity more visible within the equations. Extending the integral to $t = -\infty$ means that any transient behaviour such as the initial build-up of the grating is neglected and that we consider only the stationnary periodic response of the crystal. Making the transformation: $t' \rightarrow (t-t')$, in the $\int dt'$ integral of Eq. (18), we get:

$$\varepsilon_S(\mathbf{r},t) = \; e^{-\alpha(z-z_1)/2} \left[\; \varepsilon_S(x,y,z_1,t) + \int_0^\infty dt' \; \varepsilon_S(x,y,z_1,t-t') \; G(z,t') \; \right] \tag{20}$$

Here, the PR hologram is written at the retarded time $t-t'$, the retardation being $t' > 0$.

To help the following discussions, we have to notice that the first term of Eq. (20) or Eq. (18) (field E_T and complex amplitude ε_T) corresponds to the signal beam transmitted (T) through the photorefractive crystal, whereas the second term (E_D and ε_D) is the pump beam diffracted (D) by the PR hologram. We have thus:

$$\varepsilon_S(\mathbf{r},t) = \varepsilon_T(\mathbf{r},t) + \varepsilon_D(\mathbf{r},t) \tag{21}$$

$$\varepsilon_T(\mathbf{r},t) = \; e^{-\alpha(z-z_1)/2} \; \varepsilon_S(x,y,z_1,t) \tag{22}$$

$$\varepsilon_D(\mathbf{r},t) = \; e^{-\alpha(z-z_1)/2} \; \int_0^\infty dt' \; \varepsilon_S(x,y,z_1,t-t') \; G(z,t') \tag{23}$$

By developing $\varepsilon_S(x,y,z_1,t-t')$ from Eq. (17), we get:

$$\varepsilon_D(\mathbf{r},t) = \; e^{-\alpha(z-z_1)/2} \; \sum_n \int_0^\infty dt' \; \mathscr{E}_{S,\omega_n}(x,y,z_1,t-t') \; G(z,t') \; e^{j(\omega_n-\omega)(t-t')} \tag{24}$$

Equation (22) and Eq. (24) will be used later to calculate the PR signal on a photodiode. Consider now the diffracted field E_D defined similarly to E_R and E_S (see Eq. (16)) by $E_D(\mathbf{r},t) = \boldsymbol{Re}\,(\varepsilon_D(\mathbf{r},t)\; e^{j\omega t})$. We get:

#7601 - $15.00 USD Received 25 May 2005; revised 12 July 2005; accepted 29 August 2005
(C) 2005 OSA

$$E_D(\mathbf{r},t) = \mathbf{Re}\ (e^{-\alpha(z-z_1)/2}\ \sum_n e^{j\omega_n t} \int_0^\infty dt'\ \mathscr{E}_{S,\omega_n}(x,y,z_1,t-t')\ G(z,t')\ e^{-j(\omega_n-\omega)t'}) \qquad (25)$$

Equation (25), which is equivalent to Eq. (24), shows that the diffracted field E_D can be developed in a sum of Fourier components, each of them evolving at the Fourier frequency ω_n. Because of the $e^{-j(\omega_n-\omega)t'}$ factor in the $\int_0^\infty dt'$ integral, the crystal selects, through its response time that governs the evolution of $G(z,t')$, the frequency component ω_n closest to ω.

If for example $\omega \simeq \omega_1$, the sum over n (i.e. $\sum_n$ in Eq. (25)) restricts to $n=1$ (as ω_{US} is generally much greater than the inverse of the response time of the PR crystal). One select thus the ω_1 frequency component, i.e. the "tagged photons". As seen in Eq. (25), the diffracted beam E_D evolves then at the "tagged photons" frequency ω_1. If ω is not exactly equal to ω_1 (with still a difference smaller thant $1/\tau_{PR}$), the E_R versus E_S interference pattern (and thus the PR hologram) drifts continuously in phase, but the phase of the field, which is diffracted by this moving grating, do not drift (the phase evolution is exactly $e^{j\omega_1 t}$) with respect to the "tagged photons" field. This is a known property of the diffraction with a PR moving grating [29].

5. The PR signal with a photo detector of large area

To simplify the discussion, we will consider that the signal is detected by a photodiode of large area, located in the PR crystal output plane $z = z_2$. The photodiode signal S_{PD} is thus equal to the integral of $|\varepsilon_S|^2$ over the photodiode area. From Eq. (21) we get:

$$S_{PD}(t) = \int\int dx\,dy\ |\varepsilon_T(x,y,z_2,t)|^2 + |\varepsilon_D(x,y,z_2,t)|^2 + [\,\varepsilon_T(x,y,z_2,t)\ \varepsilon_D{}^*(x,y,z_2,t) + \text{c.c.}] \qquad (26)$$

where c.c. means the complex conjugate.

To get a sensitive detection we will modulate the amplitude, or the phase of the ultrasonic wave, and we will consider mainly the time varying component of S_{PD}. Because the acoustic wave do not change the total number of scattered photons (i.e. "tagged" + "un tagged"), the $|\varepsilon_T|^2$ term of Eq. (26) do not depend on the acoustic wave modulation. This term can thus be discarded. Since the PR gain is supposed to be quite low ($\eta_{PR} = \gamma(z_2-z_1) \ll 1$), the $|\varepsilon_D|^2$ term is much lower than the $\varepsilon_T\ \varepsilon_D{}^*$ cross term. Moreover, the $|\varepsilon_D|^2$ term builds up slowly, in a time τ_{PR} (see Eq. (19)), which can be much larger than the modulation period. The $|\varepsilon_D|^2$ term can thus be discarded too.

As in many PR experiments [18, 30, 31], we will consider thus only the $\varepsilon_T\ \varepsilon_D{}^*$ cross term, which is the product of the amplitude $\varepsilon_D{}^*$, which builds up slowly (in τ_{PR}), with the transmitted amplitude ε_T, which can vary very fast, since it is directly related to the $\varepsilon_S(x,y,z_1,t)$ source term.

By using Eq. (22) and Eq. (23), we get for the cross term photodiode signal $S_{PD} = c.c. + \int\int dx\,dy\ \varepsilon_T\ \varepsilon_D{}^*$:

$$S_{PD}(t) = c.c. + e^{-\alpha(z_2-z_1)} \int\int dx\,dy\ \varepsilon_S(x,y,z_1,t) \int_0^\infty dt'\ \varepsilon_S{}^*(x,y,z_1,t-t')\ G^*(z,t') \qquad (27)$$

To keep full generality, we have introduced here G^* although G is supposed to be real. Developing ε_S in Fourier components $\mathscr{E}_{S,\omega_n}$ with Eq. (17), and $\mathscr{E}_{S,\omega_n}$ in travel pathes field components $\mathscr{E}_{S,i,\omega_n}$ with Eq. (13), we get:

$$\begin{aligned} S_{PD}(t) = c.c. + e^{-\alpha(z_2-z_1)} \int\int dxdy \sum_{n,n'} \sum_{i,i'} \mathscr{E}_{S,i,\omega_n}(x,y,z_1,t)\ e^{j(\omega_n-\omega)t} \\ \int_0^\infty dt'\ G^*(z,t')\ \mathscr{E}_{S,i',\omega_{n'}}{}^*(x,y,z_1,t-t')\ e^{-j(\omega_{n'}-\omega)(t-t')} \end{aligned} \qquad (28)$$

#7601 - $15.00 USD Received 25 May 2005; revised 12 July 2005; accepted 29 August 2005
(C) 2005 OSA

Equation (28) is the main equation of this paper. It handles all the complexity of the PR signal, since it involves a double summation of the travel pathes (i.e. $\sum_{i,i'}$), a double summation over the Fourier components (i.e. $\sum_{n,n'}$), a double space integral over the photodiode area (i.e. $\int\int dx\,dy$), and a time integral over the retardations t' (i.e. $\int dt'$). Our first task is to simplify it.

Consider first the $\int\int dx\,dy\ \mathscr{E}_{S,i,\omega_n}(\ldots)\ \mathscr{E}_{S,i',\omega_{n'}}{}^*(\ldots)$ terms of Eq. (28). By developing $\mathscr{E}_{S,i,\omega_n}$ with Eq. (12) we get:

$$\begin{aligned}\int\int dxdy\ \mathscr{E}_{S,i,\omega_n}(\mathbf{r},t)\ \mathscr{E}_{S,i',\omega_{n'}}{}^*(\mathbf{r},t-t') = {} & J_n(\beta_i(t))\ J_{n'}(\beta_{i'}(t-t')) \\ \times\ e^{jn(\phi_i(t)+\pi/2)}\ e^{-jn'(\phi_{i'}(t-t')+\pi/2)} & \int\int dxdy\ a_i(\mathbf{r})\ a_{i'}(\mathbf{r})\ e^{-j(\theta_i(\mathbf{r})-\theta_{i'}(\mathbf{r}))}\end{aligned} \tag{29}$$

As mentioned above, due to the speckle character of the scattered field E_S, θ_i varies very fast with $\mathbf{r}=(x,y,z_1)$. As a consequence, in Eq. (29), the x,y integral of $e^{-j(\theta_i-\theta_{i'})(\mathbf{r})}$ yields zero, when $i\neq i'$. In Eq. (28), one can thus restrict the i,i' summation to the $i=i'$ terms.

This approximation is very common in optics. In Eq. (27) the $\varepsilon_S(t)\varepsilon_S{}^*(t-t')$ terms corresponds to a field intensity (or more exactly to a time correlation intensity), which must be summed over the photodiode area. Because of the spatial integral for the intensity, one can neglect the speckle interference terms, which correspond in Eq. (28) to $i\neq i'$.

For $i=i'$, consider now the $\sum_i\ \mathscr{E}_{S,i,\omega_n}(\ldots)\ \mathscr{E}^*{}_{S,i,\omega_{n'}}(\ldots)$ term of Eq. (28). By developing $\mathscr{E}_{S,i,\omega_n}$ using Eq. (12) we get:

$$\sum_i \mathscr{E}_{S,i,\omega_n}(\mathbf{r},t)\ \mathscr{E}^*{}_{S,i,\omega_{n'}}(\mathbf{r},t-t') = \sum_i\ a_i{}^2(\mathbf{r})\ J_n(\beta_i(t))\ J_{n'}(\beta_i(t-t'))\ e^{j(n\phi_i(t)-n'\phi_i(t-t'))} \tag{30}$$

Since the phase ϕ_i is randomly distributed with equal probability in the $[0,2\pi]$ interval, the factor $e^{j(n\phi_i-n'\phi_i)}$ is random, if $n\neq n'$. The Eq. (30) summation over i then yields zero. Contrarily, the $n=n'$ terms adds coherently, since $\phi_i(t)$ is strongly correlated with $\phi_i(t-t')$: ϕ_i do not depends on time, if the US beam is constant. In Eq. (28), one can then restrict the n,n' summation to the $n=n'$ terms. As a consequence, in Eq. (28), there is no $n=0$, $n'=1$ terms, which oscillates at the US frequency ω_{US}, i.e. like $e^{j(\omega_0-\omega)t}\ e^{-j(\omega_1-\omega)(t-t')}=e^{-j\omega_{US}t}\times\ldots$ (and no $n=1$, $n'=0$ terms, which oscillates like $e^{j\omega_{US}t}\times\ldots$).

All these simplifications result from incoherent character of the "tagged" versus "un tagged" speckle fields $\mathscr{E}_{S,\omega_0}$ and $\mathscr{E}_{S,\omega_1}$ described at the end of section 3. If for example one selects the "tagged photon" by making $\omega\simeq\omega_1$, the diffracted field E_D, whose frequency is ω_1, match the "tagged photon" field. The "un tagged photons" field, whose frequency is ω_0, cannot thus interfere coherently with E_D, since both fields are spatially incoherent. The photodiode signal at $\omega_1-\omega_0=\omega_{US}$ is thus very low.

Making $i=i'$ and $n=n'$, and developing $\mathscr{E}_{S,i,\omega_n}$ with Eq. (12), Eq. (28) can be rewritten in a form that will be useful for the following discussion:

$$\begin{aligned}S_{PD}(t)=c.c.+e^{-\alpha(z_2-z_1)}\int\int dxdy\sum_{n,i}a_i^2(x,y,z_1)J_n(\beta_i(t))e^{jn\phi_i(t)} \\ \int_0^\infty dt'J_n(\beta_i(t-t'))e^{-jn\phi_i(t-t')}G^*(z_2,t')e^{j(\omega_n-\omega)t'}\end{aligned} \tag{31}$$

Because of the time integral $\int_0^\infty dt'$ with the $G(z_2,t')$ kernel, one has to tune (to get a non zero signal) the pump beam frequency ω to be nearly resonant with the one of Fourier component ω_n, with practically $n=0$ or $n=1$. In that case, in Eq. (31) the summation over n can be restricted to the $n=0$ or to the $n=1$ term.

#7601 - $15.00 USD Received 25 May 2005; revised 12 July 2005; accepted 29 August 2005
(C) 2005 OSA

6. Examples of modulation of the US

As mentioned above, to get a sensitive detection, the ultrasonic wave, must be modulated with time, in amplitude or phase.

In the following, we will consider a $[0,1]$ amplitude modulation (AM), or a $[0,\pi]$ phase modulation. We will call x the cyclic ratio $(0 < x < 1)$, and $\omega_{mod} = 2\pi/T$ the modulation frequency. In both cases, the modulation can be accounted by making the change :

$$\mathscr{U}_{PZT}(t) \rightarrow \mathscr{U}_{PZT}\ H_{XX}(t)\ e^{j\psi_{XX}(t)} \tag{32}$$

where H_{XX} is a periodic function of period T, with $XX = AM$ (or PM) for amplitude (or phase) modulation, defined as :

$$\begin{array}{l} H_{AM}(t) = 1\ ;\ \psi_{AM}(t) = 0 \quad \text{for} \quad 0 < t < x\,T \\ H_{AM}(t) = 0\ ;\ \psi_{AM}(t) = 0 \quad \text{for} \quad x\,T < t < T \end{array} \tag{33}$$

$$\begin{array}{l} H_{PM}(t) = 1\ ;\ \psi_{PM}(t) = 0 \quad \text{for} \quad 0 < t < x\,T \\ H_{PM}(t) = 1\ ;\ \psi_{PM}(t) = \pi \quad \text{for} \quad x\,T < t < T \end{array} \tag{34}$$

We will consider that the modulation period T is large (typically $T \sim 1ms$) with respect to the US propagation time through the medium ($\sim 100\mu s$). All the scatterers see then the same modulation factor $H_{XX}(t)$. One can make thus the transform: $\delta s_{i,j}(t) \rightarrow H_{XX}(t)e^{j\psi_{XX}(t)}\ \delta s_{i,j}$, for the individual scattering event in Eq. (8). The inclusion of the modulation terms allows then to make in Eq. (31) the following replacements :

$$\beta_i(t) \rightarrow H_{XX}(t)\beta_i \qquad\qquad \phi_i(t) \rightarrow \phi_i + \psi_{XX}(t) \tag{35}$$

Consider first a phase modulation (PM) of the US characterized by Eq. (34) with a reference beam tuned at the US first sideband frequency ($\omega = \omega_1$); it means that we detect the "tagged" photons and thus the summation in Eq. (31) reduces to the $n = 1$ term. To simplify the analysis we consider here, and in all the other modulations examples, that the modulation is fast ($\omega_{mod}\tau_{PR} \gg 1$), and that the US excitation is low ($\beta_i \ll 1$).

For such a fast modulation, the time integral term ($\int dt' ...$) of Eq. (31), that describes the writing of the PR crystal is proportional to the average grating depth, *i.e.* to $< H_{PM}(t)\ e^{j\psi_{PM}t} >_t = 1 - 2x$ (where $< .. >_t$ is the time average operator). The signal delivered by the detector writes then :

$$S_{PD}(t) = c.c. + (1-2x)\,A\,e^{j\psi_{PM}(t)} \tag{36}$$

$$A = \eta_{PR}\ e^{-\alpha(z_2-z_1)}\ \times\ \left[\sum_i\ {J_1}^2(\beta_i)\ \int\int dx\,dy\ \ {a_i}^2(x,y,z_1)\right] \tag{37}$$

Equation (36) shows that photodiode signal exhibits the same rectangular phase change as the US phase.

We can notice that ${J_1}^2(\beta_i)\ {a_i}^2(x,y,z_1)$ is the scattered intensity, along the travel path i, at the frequency ω_1, at the location (x,y,z_1). The average value of ${J_1}^2(\beta_i)$ thus represents the ω_1 *tagged-photons* relative weight. By using the heterodyne holographic method [10, 16], we have measured this weight in similar acoustic pressure conditions : we got ${J_1}^2(\beta_i) \simeq {\beta_i}^2/4 \sim 1\%$. The signal is quadratic with pressure, and linear in acoustic energy (β_i is proportional to the pressure).

The ${J_1}^2(\beta_i)$ dependence of the interference signal can be simply understood as follows : when the reference beam is shifted from the US frequency, only *tagged-photons* at ω_{US} can built up a grating within the crystal, proportional to the modulation depth of the interference pattern, e.g proportional to the *tagged-photons*, and thus to $J_1(\beta_i)$, because the *flux* from the

#7601 - $15.00 USD Received 25 May 2005; revised 12 July 2005; accepted 29 August 2005
(C) 2005 OSA

reference field is dominant. The reference beam diffracts then a field proportional to this index grating, and the *flux* onto the detector exhibits such a ${J_1}^2(\beta_i)$ a dependence.

We can now develop the interference signal in harmonic components versus ω_{mod}, omitting the various static components. We get then :

$$S_{PD}(t) = \; - \; [\, 8x(1-2x)A\, sinc(\pi x)\,]\; cos(\omega_{mod}t - \pi x) \;+\; harmonics \tag{38}$$

Consider now the case of an amplitude modulation (AM) of the US with a reference beam at $\omega = \omega_0$. We detect the "un tagged" photons ($n = 0$ in Eq. (31)). Since $\beta_i \ll 1$, we can replace J_0 by one, in the $\int dt'$ integral of Eq. (31). Once again, the time-varying contribution gives then :

$$S_{PD}(t) = -\left[c.c. + H_{AM}(t)\, A'\right] \tag{39}$$

$$A' = \eta_{PR}\, e^{-\alpha(z_2-z_1)} \times \left[\sum_i \; (\; 1 - J_0(\beta_i))\; \int\int dx\, dy\; \; a_i^2(x,y,z_1)\right] \tag{40}$$

Here, $A' \simeq A$ since $(1-J_0) \simeq {J_1}^2$ for small argument β_i. Here there is no dependance of the signal amplitude (maximum to minimum) with the cyclic ratio x, because the PR hologram is written by the "un tagged" photons (which remains roughly constant since $\beta_i \ll 1$). The PR signal observed here has the same order of magnitude than for PM modulation, but the signal sign is reversed. This is expected. The total number of photons ("un tagged" + "tagged") do not depend on the US. Here, we detect the "un tagged" photon ($\omega = \omega_0$), and the signal is maximum, when the US is off (no tagged photons). In the PM modulation previous case, we have detected the "tagged photon", and the signal was maximum, when the US was on. The two situations ($\omega = \omega_0$ or $\omega = \omega_1$) can be viewed as an *absorption-like* detection (bright background), or an *emission-like* detection (dark background) respectively.

By developing the signal in harmonic components, we get:

$$S_{PD}(t) = -\left[\, 4A'x\;\; sinc(\pi x)\,\right]\;\; cos(\omega_{mod}t - \pi x) \;+\; harmonics \tag{41}$$

Consider finally the case of an amplitude modulation (AM) with a reference beam at $\omega = \omega_1$. We get then for the signal shape versus time:

$$S_{PD}(t) = c.c. + x\, H_{AM}(t)\, A \tag{42}$$

where A is given by Eq. (37). Here again the average "tagged photon" field yields to the x proportionality factor of Eq. (42), since $x = < H_{AM}(t)\; e^{j\psi_{AM}t} >_t$. The development in harmonic components is:

$$S_{PD}(t) = \;\left[\, 4Ax^2\; sinc(\pi x)\,\right]\; cos(\omega_{mod}t - \pi x) \;+\; harmonics \tag{43}$$

7. Experimental results and discussion

The PR interferometric setup is similar to the one previously described [12] (see Fig. 3). The PR crystal is a single crystal of undoped GaAs grown by Liquid Uncapsulated Czochralski method. The crystal is oriented in an energy transfer configuration [22,23] with (110), $(1-10)$ and (001) faces. The signal and the reference beams enter both along the (110) (*co-directional type*) face or enter respectively on the (110) and (001), in order to reduce pump scattering onto the detector (*orthogonal-type* configuration). The orthogonal configuration is surely not suitable for media that exhibit fast speckle decorrelation time : in such a case the related τ_{PR} time establishment can be long (some tens of *ms* - depending on the inverse of the average *flux*) due to a higher spatial frequency of the fringes within the crystal. We used two single frequency

#7601 - $15.00 USD Received 25 May 2005; revised 12 July 2005; accepted 29 August 2005
(C) 2005 OSA

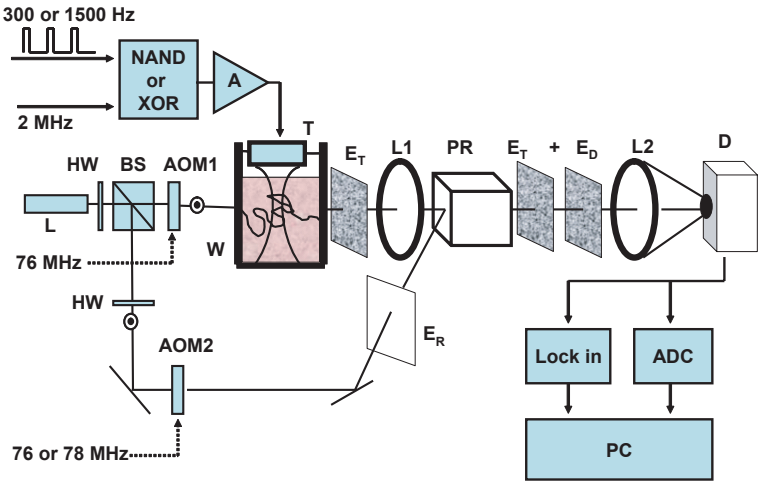

Fig. 3. Experimental setup. L: 1064*nm* single axial mode YAG: Nd^{3+} laser. HW:half-wave optical plates. BS : polarisation cube beam-splitter. A: US power amplifier. T: 2*MHz* US piezo-transducer. AOM1,2: Acousto-optic modulators. E_T, E_D : fields associated to the speckle wavefronts (see text). E_R plane wave reference field. D: InGaAs photodetector ($\phi = 5mm$) + transimpedance amplifier. L1,2 : wide aperture aspherical lenses. W: water tank+scatterring media. PR: GaAs photorefractive crystal. Measurements are performed either with a lock-in detection or an ADC analog to digital converter (16*bits*, 48*kHz*) and recorded by a PC computer.

$YAG : Nd^{3+}$ lasers (1200*mW*, *Crystal Laser corp.* and 120*mW*, *LightWave electronics corp.*), vertically polarized and operating at 1064*nm*. The present setup is not yet fully optimized in *flux*, especially because of the presence of the acousto-optical modulators on the arms of the interferometer that introduce many losses. Most of the experimental results presented here have been performed with the 120*mW* source. The intensity used with the two sources depend on the sample, they varies typically between $10mW/cm^2$ and $70mW/cm^2$, which is beneath safety regulations for *invivo* imaging. The intensity of the reference beam (onto the crystal) can vary between $25mW/cm^2$ and $200mW/cm^2$. Evidently, the configuration using the 1200*mW* source is able to provide a faster built up of the photorefractive effect. The detector is a large area InGaAs ($\phi = 5mm$) photodiode (*Hamamatsu corp.*) mounted on a high pass two-stages amplification in order to favor the *ac* component compared the *dc* one. The first stage is low bias current (OPA111) transimpedance amplifier ($R = 10^6\Omega$).

The transducer (T) (*Panametrics*, focal length=68 mm, Diameter=40mm) operates in *cw* mode at $\omega_{US} = 2MHz$ with a maximum pressure of 1*MPa* at focus, corresponding to a 35*V* peak-to-peak excitation. The ω_{US} signal is amplitude or phase modulated at 300 or 1500*Hz* by using an NAND or XOR logical gate (74LS00 or 74LS86) followed by a US power amplifier (SCD Nuclétudes 2.30.30A : 10*W*). The respective frequencies of the signal (ω_0) and reference (ω) beams can be freely adjusted using acousto optic modulators (AOM1,2 : *Crystal Technologies*) in order to perform detection with $\omega = \omega_0$ ($\omega_{AOM1,2} = 76MHz$) or with $\omega = \omega_1$ ($\omega_{AOM1} = 76MHz$, $\omega_{AOM2} = 78MHz$).

The signal can be recorded either with a lock-in detection (*EG&G* instruments 7260 digital model), or with an analog to digital converter with *16bits* resolution working at a rate of *48kHz* : in this configuration, the signal is recorded during *1.5s* and we perform a Fast Fourier Transform (FFT) in order to extract the magnitude of the signal at the modulation frequency, and to

#7601 - $15.00 USD Received 25 May 2005; revised 12 July 2005; accepted 29 August 2005
(C) 2005 OSA

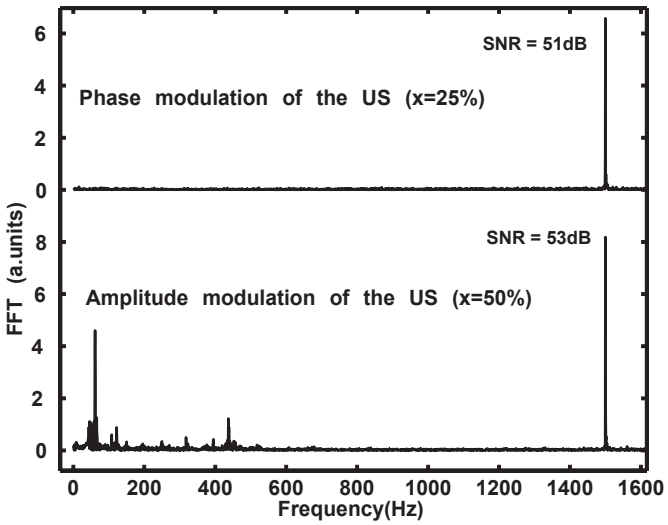

Fig. 4. Fast Fourier transform of a typical acousto-optical signal issued from a $10cm$ thick scattering (intralipid+water) solution recorded with a ($16bits$, $48kHz$) analog to digital converter in the case of a phase (cyclic ratio 25%) or amplitude (cyclic ratio 50%) modulation of the US at $1500Hz$. The power *SNR* is given at the first harmonics of the modulation frequency.

get an estimation the signal-to-noise ratio (*SNR*). Figure 4 shows the Fourier spectrum of the signal with intralipid solution, at maximum response for amplitude and phase modulation of the US at $1500Hz$, e.g with a cyclic ratio respectively of 50% and 25%. These spectra exhibit a comparable power *SNR* ($53dB$ for the amplitude modulation, and $51dB$ for the phase modulation), but the amplitude modulation case contains an important noise at low frequency : this is not surprising since the grating is built-up with the *un-tagged* photons, and the interference pattern is more sensitive to technical noise of the setup.

Test experiments of the acousto-optical response have been performed either with a $e = 2cm$ thick chicken breast sample, or with a $e = 10cm$ liquid scattering sample (intralipid aqueous solution). We have at first measured with a lockin detection, at fixed pressure and light *flux*, in the intralipid sample, and for the various modulation, the response of the AO signal, which is described in section 7.2, as a function of the cyclic ratio x. Figure 5 shows the comparison between the experimental data, and the corresponding fit deduced from Eq. (38), Eq. (41) and Eq. (43). The agreement validates our theoretical analysis, and the $S_{PD}(t)$ expressions.

As a final test of our model, Fig. 6 shows the magnitude of the AO signal as a function of the acoustic pressure ($\propto \mathscr{U}_{PZT}$), with the chicken sample, and the corresponding fit. Measurements are performed with amplitude and phase modulation (AM and PM) of the US excitation. For the AM case, the cyclic ratio is of $x = 1/2$, and the reference beam frequency is $\omega = \omega_0$ (detection of the "un tagged photons" at the US carrier frequency). For the PM case, $x = 1/8$ and $\omega = \omega_1$ (detection of the "tagged photons" at the US first sideband frequency). These measurements exhibit a quadratic response with a comparable magnitude, as expected by the model when the acoustic pressure excitation is weak, since $J_1^2(x) = 1 - J_0(x) \simeq x^2/4$ for a small x argument. Moreover, we measure in this case a ratio $S_{AM}/S_{PM} \simeq 1.74$: this is fully compatible with the results shown on Fig. 5, for the case of a weak acoustic pressure perturbation.

#7601 - $15.00 USD Received 25 May 2005; revised 12 July 2005; accepted 29 August 2005
(C) 2005 OSA

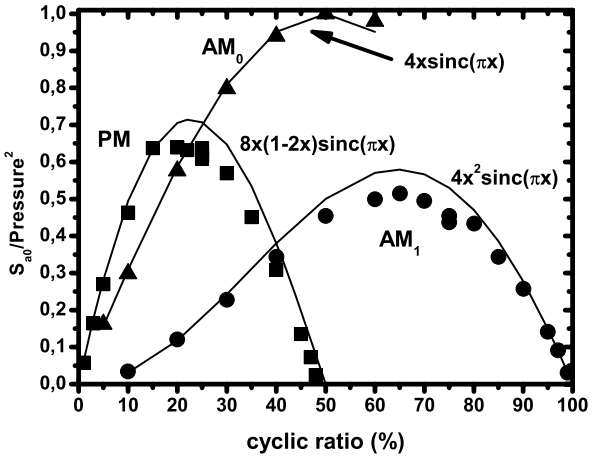

Fig. 5. Dotted : Quadratic pressure normalized response as a function of the cyclic ratio x of the acousto optical signal for phase modulation (PM), amplitude modulation (AM_0) and amplitude modulation + shift of the US frequency (AM_1). Line : associated fit.

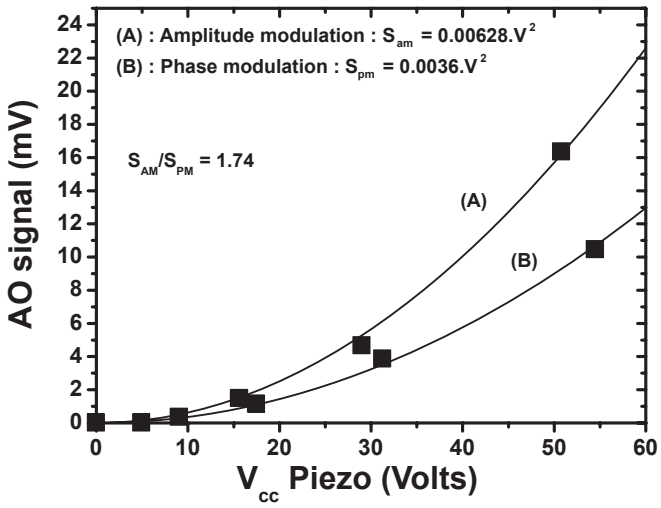

Fig. 6. Comparison of the normalised experimental (square) and theoretical AO response for an amplitude (A) and a phase (B) modulation of the US in the low acoustic pressure regime (proportional to the peak to peak excitation V_{cc} of the US emitter) pressure. The cyclic ratio is $x = 1/2$ in case (A) and $x = 1/8$ in case (B), with a frequency modulation of $305Hz$. The 1.74 ratio is compatible with the calculated magnitudes associated these modulations.

#7601 - $15.00 USD Received 25 May 2005; revised 12 July 2005; accepted 29 August 2005
(C) 2005 OSA

In these test experiments, we have not tried here to minimize τ_{PR}, but preliminary results show that a co-directional beam coupling with a pump beam of $150mW$ generates a $\tau_{PR} \sim 1ms$.

8. Conclusion

In this paper, we have presented, and verified experimentally, a model of the *real-time* acousto optical response for thick highly scattering media when coupled to an interferometric setup using a photorefractive (PR) crystal as recombination plate. We have shown that the various speckle patterns associated to the sidebands generated by the acousto optical effect are not correlated. By choosing the frequency of the PR pump beam, we are able to select the acousto optic component that builds up the PR hologram (”un tagged” photon for a pump beam at the carrier frequency [11], or ”tagged photons” for a pump beam at the US sideband frequency [12]). The PR effect selects thus the specified acousto optic component, that can be easily detected by a proper amplitude or phase modulation scheme.

The agreement of predictions the theoretical model with the experimental results is excellent. As predicted by the model, and as seen experimentally, the modulation signals obtained for both ”tagged” and ”un tagged photon” detection have almost the same order of magnitude. The response of the system *versus* the acoustic pressure reveals also a quadratic variation (linear in acoustic power) for *untagged-photons* and *tagged-photons* shifted from the US frequency. This confirms that the perturbation brought by the US is weak.

A careful study of the PR time response needs further to be performed, in order to find suitable conditions for *in vivo* measurements, *e.g* faster than the speckle decorrelation time.

#7601 - $15.00 USD Received 25 May 2005; revised 12 July 2005; accepted 29 August 2005
(C) 2005 OSA